

Evolution of the Fermi surface of the nematic superconductors $\text{FeSe}_{1-x}\text{S}_x$

A. I. Coldea,^{1,*} S. F. Blake,¹ S. Kasahara,² A. A. Haghighirad,¹ M. D. Watson,^{1,3} W. Knafo,⁴ E. S. Choi,⁵ A. McCollam,⁶ P. Reiss,¹ T. Yamashita,² M. Bruma,¹ S. Speller,⁷ Y. Matsuda,² T. Wolf,⁸ T. Shibauchi,⁹ and A. J. Schofield¹⁰

¹*Clarendon Laboratory, Department of Physics, University of Oxford, Parks Road, Oxford OX1 3PU, UK*

²*Department of Physics, Kyoto University, Kyoto 606-8502, Japan*

³*Diamond Light Source, Harwell Campus, Didcot, OX11 0DE, UK*

⁴*Laboratoire National des Champs Magnétiques Intenses (LNCMI-EMFL),*

UPR 3228, CNRS-UJF-UPS-INSA, 143 Avenue de Rangueil, 31400 Toulouse, France

⁵*National High Magnetic Field Laboratory, Florida State University, Tallahassee, FL 32310, USA*

⁶*High Field Magnet Laboratory (HFML-EMFL), Radboud University, 6525 ED Nijmegen, The Netherlands*

⁷*Department of Materials, University of Oxford, OX1 3PH, UK*

⁸*Institut für Festkörperphysik, Karlsruhe Institute of Technology, 76021 Karlsruhe, Germany*

⁹*Department of Advanced Materials Science, University of Tokyo, Kashiwa, Chiba 277-8561, Japan*

¹⁰*School of Physics and Astronomy, University of Birmingham, Edgbaston, Birmingham B15 2TT, UK*

(Dated: November 23, 2016)

We investigate the evolution of the Fermi surfaces and electronic interactions across the nematic phase transition in single crystals of $\text{FeSe}_{1-x}\text{S}_x$ using Shubnikov-de Haas oscillations in high magnetic fields up to 45 tesla in the low temperature regime. The unusually small and strongly elongated Fermi surface of FeSe increases monotonically with chemical pressure, x , due to the suppression of the in-plane anisotropy except for the smallest orbit which suffers a Lifshitz-like transition once nematicity disappears. Even outside the nematic phase the Fermi surface continues to increase, in stark contrast to the reconstructed Fermi surface detected in FeSe under applied external pressure. We detect signatures of orbital-dependent quasiparticle mass renormalization suppressed for those orbits with dominant $d_{xz/yz}$ character, but unusually enhanced for those orbits with dominant d_{xy} character. The lack of enhanced superconductivity outside the nematic phase in $\text{FeSe}_{1-x}\text{S}_x$ suggest that nematicity may not play the essential role in enhancing T_c in these systems.

Nematic electronic order is believed to play an important role in understanding superconductivity in iron-based and copper oxide superconductors [3–5]. FeSe is an ideal system to study this interplay as the nematic phase below 87 K is manifested via a strong distortion of the Fermi surface, which has been linked to the lifting of the orbital degeneracy of the Fe d_{xz}/d_{yz} bands [1] and the development of d_{xy} orbital anisotropy [6]. Another peculiarity of FeSe is the strong disparity in band renormalization between the degenerate d_{xz}/d_{yz} bands compared with a much stronger effect for the d_{xy} band, as determined from angle resolved photoemission spectroscopy (ARPES) at high temperatures [1]. In bulk FeSe, superconductivity emerges out of the electronic nematic phase [1], but its relevance for the high T_c superconductivity found under applied pressure, intercalation or by surface doping, remains unclear [7–9]. One approach in finding the interplay between nematicity and superconductivity is using chemical pressure induced by isoelectronic substitution in $\text{FeSe}_{1-x}\text{S}_x$, which dramatically suppresses the nematic phase [2].

Chemical pressure may mimic the behaviour of applied hydrostatic pressure by bringing the FeSe layers closer together, potentially increasing the bandwidth and suppressing the electronic correlations. Thus, isoelectronic substitution in superconducting $\text{FeSe}_{1-x}\text{S}_x$ is an alternative tuning parameter which may provide new insight into the interplay of the nematic order found in the parent compound, and the induced magnetic order and enhanced superconductivity found under physical pressure [10–12]. In this paper we use quantum oscillations in a series of sulphur-substituted FeSe single crystals to probe in detail the evolution of complex Fermi surfaces

and quasiparticle properties across the putative nematic quantum phase transition at very low temperatures and high magnetic fields. Samples were grown by the KCl/AlCl₃ chemical vapour transport method, and their compositions were determined using EDX measurements. Magnetotransport measurements were performed in high magnetic fields up to 45 T at NHMFL in Tallahassee and up to 33 T at HFML in Nijmegen at low temperatures down to 0.35 K using ³He cryogenic systems.

Quantum Oscillations in $\text{FeSe}_{1-x}\text{S}_x$. Fig. 1 shows resistivity measurements of $\text{FeSe}_{1-x}\text{S}_x$ in magnetic fields up to 45 T and at low temperatures ($T \sim 0.4$ K), with the magnetic field either perpendicular to the highly conducting ab layers ($B \parallel c$, $\theta=0$) or tilted away by an angle ($\theta=30^\circ$). The upper critical field for the transition from the superconducting to the normal state in $\text{FeSe}_{1-x}\text{S}_x$ reaches a maximum of about 20 T ($x \sim 0.07(1)$ for $B \parallel c$) and it varies with composition in a similar way as T_c , which has a maximum of about 11(1) K for the same composition, as shown in the phase diagram in Fig.3a. In the normal state, we observe Shubnikov-de Haas oscillations superimposed on the transverse magnetoresistance signal, with different samples showing dominance of different frequencies due to the multiple electronic bands involved across the compositional range. The quantum oscillations are periodic in $1/B$ and this is clearly visualized after removing a polynomial background magnetoresistance, as shown in Fig.1b. Quantum oscillations are a bulk probe of the size and shape of the Fermi surface, by measuring extremal cross-sectional orbits with a high accuracy of up to $\sim 0.04\%$ of the area of the first Brillouin zone. The extremal areas of

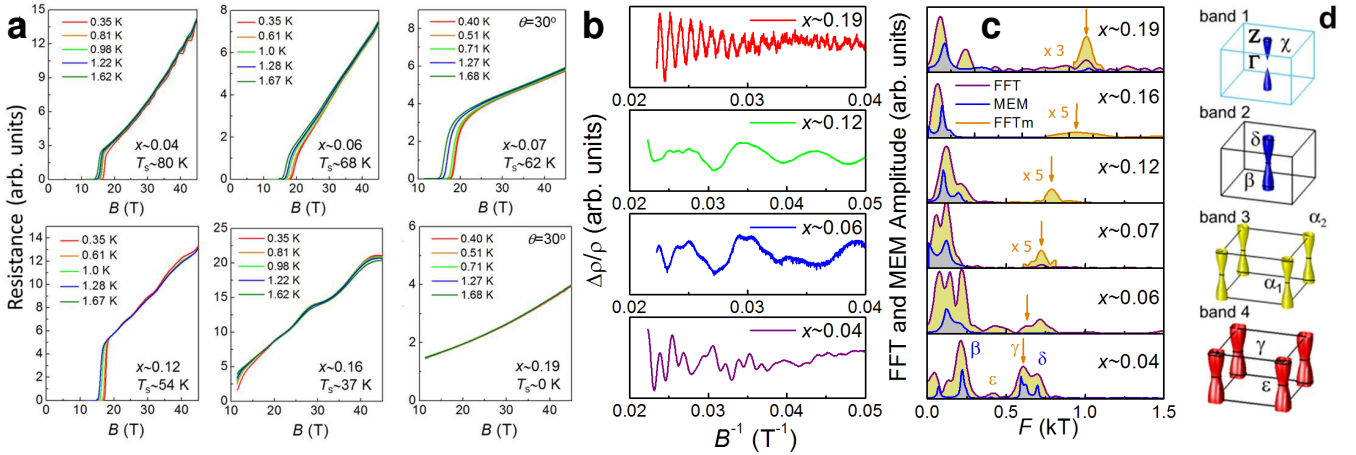


FIG. 1. **Quantum oscillations in superconducting single crystals of $\text{FeSe}_{1-x}\text{S}_x$.** **a**, The in-plane resistance $R_{xx}(B)$ as a function of magnetic field B for different compositions, x and T_s . Measurements were performed at constant low temperatures between 0.3-2 K by sweeping the magnetic fields up to 45 T with $B||c$ axis ($\theta=0$) or $\theta = 30^\circ$ for $x=0.19$ and $x=0.07$. **b**, The oscillatory part of the resistivity $\Delta\rho_{osc}/\rho$ obtained by removing a polynomial background from the raw data in a) at the lowest measured temperature. **c**, The frequency spectra obtained using a fast Fourier transform (FFT) and maximum entropy method (MEM). A multiplied FFT spectrum is used to emphasize the high frequency features with their positions indicated by vertical arrows. **d**, The proposed Fermi surface and the different extremal areas for $\text{FeSe}_{1-x}\text{S}_x$ obtained by shrinking the calculated Fermi surface in the tetragonal phase by more than 150 meV [1, 2] (see also Supplemental Material). Frequencies below 200 T cannot be reliably assigned due to a possible overlap of at least 3 different small frequencies (α_1 , α_2 and χ).

the Fermi surface normal to the applied magnetic field are obtained from the Onsager relation, $F_i = A_{k_i} \hbar / (2\pi e)$, as each pocket can contribute two extremal orbits to the quantum oscillation signal (minimum at $k_z=0$ and maximum at $k_z=\pi/c$) [13].

The low-temperature experimental Fermi surface of FeSe is that of a multi-band system, being composed of small and anisotropically distorted quasi-two dimensional electronic bands, one hole and two electron bands [1], with the smallest electron bands showing unusually high mobility [14, 15]. The fast Fourier transform (FFT) spectra of such a complex Fermi surface could have up to six different frequencies, with two different frequencies, respectively, associated with the minimum and maximum extremal orbits of each quasi-two dimensional cylindrical Fermi surface. Fig.1c shows the FFT spectrum at low concentrations ($x \sim 0.04$) for $\text{FeSe}_{1-x}\text{S}_x$, which is quite similar to previous studies on FeSe [1, 16] displaying many frequencies, labelled as α , β , γ and δ , ϵ , all below 800 T. This suggests that each pocket of the Fermi surface corresponds to a very small fraction of $\sim 2\%$ of the basal plane area of the Brillouin zone (see Fig.1d) and these pockets areas are a factor ~ 5 smaller than those predicted by the band structure calculations (see Fig.SM7 in Supplemental Material (SM)). The observed frequencies for $x \sim 0.04$ are associated with the corrugated hole-like cylinder, with extremal areas β (214 T) and δ (690 T) and two electron-like pockets that have very different quasiparticle effective masses. The outer electron cylindrical band with dominant d_{xy} character has a maximum extremal orbit, γ (~ 609 T), and a possible minimum orbit ϵ (~ 440 T) which has a similar mass of $\sim 6m_e$

to γ , and it is unlikely to be a second harmonic of β (see Fig. SM4). The inner small electron band, pocket α , should also be a cylinder with two possible orbits α_1 and α_2 , as drawn in Fig.1d). However, these low frequencies are often difficult to distinguish in the FFT spectra of FeSe and their signatures can be seen below 200 T in Fig.1c, where both the polynomial background as well as $1/f$ noise can generate artificial peaks. This small α pocket is expected to have a light mass and high mobility [14].

With increased sulphur substitution around $x \geq 0.12$, the observed magnetoresistance is indeed dominated by a low frequency, which decreases from 120(5) T for $x \sim 0.12$ to 67(5) T for $x \sim 0.16$ and around 35(5) for $x \sim 0.17$, as seen in Fig.1a and Fig.SM3. An unusual feature of this small pocket for $x \sim 0.16$ is its non-trivial Berry phase and a lighter mass ($\sim 1.7(1) m_e$), which may originate from a Dirac-like dispersion of a small electronic band (α_1 or α_2 in Fig.1d) which would disappear outside the nematic phase [19]. On the other hand, this prominent low frequency could also originate from the inner hole band centered at the Z point (χ in Fig.1d), which was detected in ARPES studies for $x \sim 0.12$, once the orbital ordering is reduced by the sulphur substitution [2]. The high frequencies of the outer electron and hole bands (γ and δ , respectively) increase monotonically with x , even outside the nematic phase as shown in Fig. 1c, implying that there is no Fermi surface reconstruction induced by chemical pressure due to the lack of a magnetic phase outside the nematic phase, in contrast to the studies on FeSe under applied pressure [8]. Instead, our quantum oscillation data for $\text{FeSe}_{1-x}\text{S}_x$ may suggest that a Lifshitz-like transition may take place as we ob-

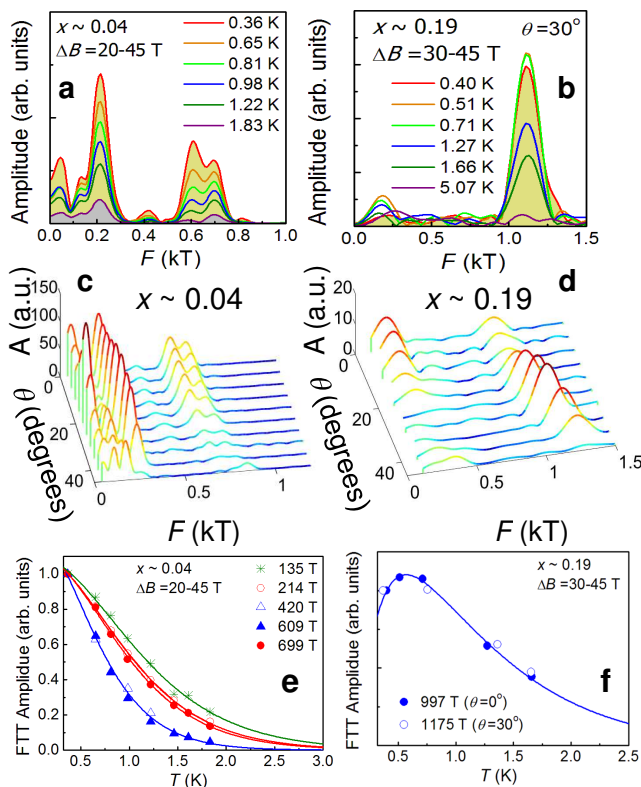


FIG. 2. **Quasiparticle effective masses of $\text{FeSe}_{1-x}\text{S}_x$.** a, b Temperature-dependence of the Fourier transform (FFT) amplitude of different frequencies for two different compositions, $x \sim 0.04$ with $T_s \sim 80$ K and $x \sim 0.19$, which is outside the nematic phase. c, d The angular dependence of the FFT amplitudes showing for the highest frequency an enhanced amplitude for $x \sim 0.19$ around $\theta \sim 30^\circ$. e, f, Temperature-dependence of the amplitude of oscillation from which the effective masses is extracted using a Lifshitz-Kosevich (LK) formula [17] (solid line) for different compositions. Clear deviation from the LK formula is observed for $x \sim 0.19$ and the fit uses a two-component model, as described in Ref.[18].

serve the disappearance of a low frequency once the nematic phase is suppressed (see also Fig.3). This effect occurs when a cylindrical Fermi surface topology changes due to a strong increase of the interlayer warping. Consequently, Fermi surface becomes disconnected in the centre of the Brillouin zone and one candidate for this behaviour would be α_1 in Fig.1d. The presence of a Lifshitz-like transition on the edge of the nematic phase was previously identified in ARPES studies in electron-doped single crystals of FeSe using in-situ potassium coating [20]. A Lifshitz transition was found to coincide with the disappearance of the spin-density wave in electron-doped BaFe_2As_2 [21].

Quasiparticle effective masses. A direct manifestation of the effect of electron-electron interactions is the relative enhancement of the quasi-particle effective masses compared to the bare band mass. The cyclotron-averaged effective masses of the quasiparticles for each extremal orbit can be extracted from the temperature dependence of the amplitude of the

quantum oscillations [13], as shown in Fig.2 and Fig.SM4. For low substitution $x \sim 0.04$, the values of the effective masses are close to those reported for FeSe [16, 22]; the β and δ orbits of the outer hole band have similar effective masses $\sim 4(1) m_e$, indicating that they originate from the same band with dominant d_{xz}/d_{yz} band character at the minimum and maximum k_z locations of a corrugated quasi-two dimensional band. The γ and ϵ orbits correspond to the outer electron band with dominant d_{xy} band character, which has a particularly heavy mass of $\sim 7(1) m_e$, confirming the strong orbitally-dependent band renormalization found by ARPES studies [1].

Outside the nematic phase for $x \sim 0.19$, the background magnetoresistance is almost quadratic and we detect some frequencies below 600 T (see also Sample 2 in Fig.SM6), but only a single high frequency oscillation with a rather peculiar behaviour, as shown in Fig.2b and d. Firstly, the largest amplitude of this frequency is observed not at $\theta = 0$, as expected for a Shubnikov-de Haas signal but at $\theta = 30^\circ$ (Fig.2d). This angle is not the Yamaji angle, ($\theta_Y = 70^\circ$) [23] at which a constructive interference occurs when the minimum and maximum orbit of a quasi-two dimensional cylinder coincide [24]. Other reasons for an interference could be that coincidentally two orbits, originating either from the outer hole and electron bands, generate the same frequencies (and cannot be separated by the FFT due to limited field window) or that both frequencies originate from the same band, but are spin-split in the presence of magnetic order, as the Zeeman energy alone would not generally generate two frequencies (see also the splitting shown by the MEM spectrum in Fig.SM6). Secondly, the temperature dependence of the FFT amplitude of this high frequency (Fig.2e) drops at low temperatures (below 0.6 K), in contrast to the expected Lifshitz-Kosevich behaviour found for all frequencies for $x \sim 0.04$ (Fig.2f). This behaviour is reminiscent of the low temperature behaviour of heavy fermion systems with strongly polarized bands and close frequencies, but different effective masses [18]. Thus, to model the observed temperature dependence we use an extended Lifshitz-Kosevich formula to account for the phase difference of the two orbits [18], which gives two very different cyclotron effective mass: one lighter mass of $\sim 3.7m_e$ (dominant at high-temperature) likely assigned to the outer hole band with d_{xz}/d_{yz} character and a much heavier mass, possibly larger than $\sim 15(7)m_e$ (see the deviation of the FFT amplitude below 0.5 K in Fig.SM4). This suggest a strong mass enhancement for the outer electron band with dominant d_{xy} band character just outside the nematic phase. An alternative interpretation could be that we detect a spin-split Fermi surface in the presence of a local effective magnetic field, as in heavy fermions [18]; but as there is no magnetism detected in these materials outside the nematic phase, this scenario may be unlikely. The effective masses and electronic correlations associated to the orbits with predominant d_{xz}/d_{yz} character (outer hole band in Fig.3d) are suppressed with x (with no clear signatures of criticality), similarly to the evolution of T_c (Fig.3a), suggesting that these bands play an dominant in the pairing mechanism and their strength is reduced once the elec-

tronic bandwidth increases with chemical pressure [25].

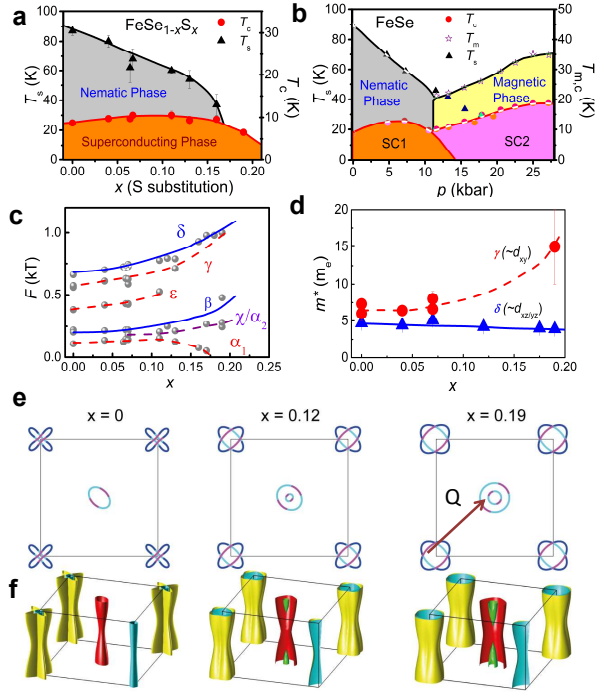


FIG. 3. Evolution of the electronic properties of $\text{FeSe}_{1-x}\text{S}_x$. a, Phase diagram of $\text{FeSe}_{1-x}\text{S}_x$ indicating the suppression of the nematic phase, (T_s , solid triangles) and the small dome of superconductivity induced by sulphur substitution, x (T_c , solid circles) using data from Fig.SM1. b, Proposed phase diagram of FeSe under pressure based on Ref. [8] showing the low T_c (SC1) and high T_c phases (SC2) as well as the new magnetic phase. c, The evolution of the observed quantum oscillations frequencies. Solid lines are the calculated frequencies for the large outer hole band based on ARPES data from Ref.[2]. The dashed lines are guides to the eye. d, The quasiparticle effective masses of the high frequencies, γ and δ . Solid and dashed lines are guides to the eye. e and f, Proposed Fermi surfaces of $\text{FeSe}_{1-x}\text{S}_x$ for different values of x as a slice at $k_z = \pi/c$ and 3D representation, respectively. A possible inter-band nesting vectors, \mathbf{Q} is also shown.

Fermi surface evolution. The evolution of the low temperature Fermi surfaces and quasiparticle masses with chemical pressure in $\text{FeSe}_{1-x}\text{S}_x$, summarized in Fig.3, suggesting a change from a three-band model for FeSe to a four-band model around $x = 0.12$, as found in ARPES studies [2]. Furthermore, once the boundaries of the nematic phase have been crossed around $x \sim 0.18(1)$, the Fermi surface suffers a Lifshitz-like transition (as the lowest frequency disappears) whereas the high frequencies corresponding to the outer electron, γ , and hole, δ , maximum orbits increase monotonically with chemical pressure, even away from the nematic phase boundaries, as shown in Fig.2b and Fig.3c. This is in contrast to the Fermi surface of FeSe under applied pressure [8], where only small frequencies were detected outside the nematic phase and were linked to a possible Fermi surface reconstruction in the presence of the new structural and magnetic phase [11, 12]. With chemical pressure, the Fermi sur-

face sheet of the outer hole band which is severely elongated for FeSe (see Fig.3e and f) becomes more isotropic. As the ellipse transform into a circle, the cross-section area of the Fermi surface increases, in agreement with the changes in the k_F values determined from ARPES studies [2] (see solid lines in Fig.3c). Additionally to the effect of nematic order on the Fermi surface, we observe that the orbits corresponding to the outer bands would continually expand with increasing x , and eventually could reach the calculated values of the same orbits of the superconductor FeS, as shown by a linear extrapolation for γ in Fig.SM7. The Fermi surfaces of $\text{FeSe}_{1-x}\text{S}_x$ being severely reduced in size compared with the prediction of band structure calculations (varying from a factor of five for FeSe towards a factor 3 around $x \sim 0.17$) is an important consequence of strong orbitally-dependent inter- and intra-band electronic interactions, significantly large in iron chalcogenides [1, 26], but also found in many iron-based superconductors [27, 28]. These effects may be suppressed once the bandwidth increases with sulphur substitution from FeSe towards FeS. The orbital-dependent mass renormalizations, in which the quasiparticle mass of the outer electron band with dominant d_{xy} orbital character (γ pocket) seems to increase with chemical pressure outside the nematic phase, whereas that of the outer hole band with mixed $d_{xz/yz}$ character (δ pocket) decreases (Fig.3b), are likely to play a different role in pairing interactions in these relatively low- T_c superconductors as well as in enhancing quantum nematic fluctuations, close to a putative nematic critical point [29, 30]. Furthermore, one can envisage that orbital-dependent effects would promote the stabilization of other competing electronic phases, as found in FeSe under pressure, but not yet revealed in $\text{FeSe}_{1-x}\text{S}_x$ up to the studied compositions.

FeSe, with a very small Fermi surface, harbours a fragile balance of competing interactions, which either distort the Fermi surface as a Pomeranchuk instability towards a nematic phase, or stabilize a spin-density wave and/or superconducting phase [31–33]. The spin fluctuations increase only at low temperature in the nematic phase of FeSe [34], but as the sizes of the outer electron and hole bands coincide outside the nematic phase in $\text{FeSe}_{1-x}\text{S}_x$, one may expect nesting and spin fluctuations may be enhanced. The fact that superconductivity is continuously suppressed with chemical pressure (Fig.3a) could imply that the nematic fluctuations are not the main factor in superconducting pairing in $\text{FeSe}_{1-x}\text{S}_x$. The low T_c superconductivity region of $\text{FeSe}_{1-x}\text{S}_x$ has the same electronic trends as those found in FeSe under pressure below 10 kbar (Fig.3b), suggesting that the high T_c superconductivity observed at high pressure may be decoupled from the nematic state of FeSe by a new structural and magnetic phase [12]. This new clean system, $\text{FeSe}_{1-x}\text{S}_x$, provides access to a nematic quantum phase transition, quite unique for iron-based superconductors, and it may help clarify the role of nematicity in relation to superconductivity and the relevance of the Lifshitz transition and orbitally-selective electronic correlations.

Acknowledgments. We thank J. C. A. Prentice for computational support, N. Davies and A. Narayanan for prelimi-

nary sample preparation and A. Chubukov and A. Shekhter for useful discussions. This work was mainly supported by EPSRC (EP/L001772/1, EP/I004475/1, EP/I017836/1). A.A.H. acknowledges the financial support of the Oxford Quantum Materials Platform Grant (EP/M020517/1). A portion of this work was performed at the National High Magnetic Field Laboratory, which is supported by National Science Foundation Cooperative Agreement No. DMR-1157490 and the State of Florida. Part of this work was supported supported by HFML-RU/FOM and LNCMI-CNRS, members of the European Magnetic Field Laboratory (EMFL) and by EPSRC (UK) via its membership to the EMFL (grant no. EP/N01085X/1). The authors would like to acknowledge the use of the University of Oxford Advanced Research Computing (ARC) facility in carrying out part of this work. AIC acknowledges an EPSRC Career Acceleration Fellowship (EP/I004475/1).

* corresponding author: amalia.coldea@physics.ox.ac.uk

- [1] M. D. Watson, T. K. Kim, A. A. Haghighirad, N. R. Davies, A. McCollam, A. Narayanan, S. F. Blake, Y. L. Chen, S. Ghanadzadeh, A. J. Schofield, M. Hoesch, C. Meingast, T. Wolf, and A. I. Coldea, *Phys. Rev. B* **91**, 155106 (2015).
- [2] M. D. Watson, T. K. Kim, A. A. Haghighirad, S. F. Blake, N. R. Davies, M. Hoesch, T. Wolf, and A. I. Coldea, *Phys. Rev. B* **92**, 121108 (2015).
- [3] R. M. Fernandes, A. V. Chubukov, and J. Schmalian, *Nature Physics* **10**, 97104 (2014).
- [4] Y. Schattner, S. Lederer, S. A. Kivelson, and E. Berg, *Phys. Rev. X* **6**, 031028 (2016).
- [5] F. Wang, S. A. Kivelson, and L. D.-H., *Nature Physics* **11**, 959963 (2015).
- [6] M. D. Watson, T. K. Kim, L. C. Rhodes, M. Eschrig, M. Hoesch, A. A. Haghighirad, and A. I. Coldea, *Phys. Rev. B* **94**, 201107 (2016).
- [7] C. H. P. Wen, H. C. Xu, C. Chen, Z. C. Huang, Y. J. Pu, Q. Song, B. P. Xie, M. Abdel-Hafiez, D. A. Chareev, A. N. Vasiliev, R. Peng, and D. L. Feng, *Nat. Commun.* **7**, 10840 (2016).
- [8] T. Terashima, N. Kikugawa, A. Kiswandhi, D. Graf, E.-S. Choi, J. S. Brooks, S. Kasahara, T. Watashige, Y. Matsuda, T. Shibauchi, T. Wolf, A. E. Böhmer, F. Hardy, C. Meingast, H. v. Löhneysen, and S. Uji, *Phys. Rev. B* **93**, 094505 (2016).
- [9] M. Burrard-Lucas, D. G. Free, S. J. Sedlmaier, J. D. Wright, S. J. Cassidy, Y. Hara, A. J. Corkett, T. Lancaster, P. J. Baker, S. J. Blundell, and S. J. Clarke, *Nature Materials* **12**, 15 (2013).
- [10] T. Terashima, N. Kikugawa, S. Kasahara, T. Watashige, T. Shibauchi, Y. Matsuda, T. Wolf, A. E. Böhmer, F. Hardy, C. Meingast, H. v. Löhneysen, and S. Uji, *Journal of the Physical Society of Japan* **84**, 063701 (2015), <http://dx.doi.org/10.7566/JPSJ.84.063701>.
- [11] S. Knöner, D. Zielke, S. Köhler, B. Wolf, T. Wolf, L. Wang, A. Böhmer, C. Meingast, and M. Lang, *Phys. Rev. B* **91**, 174510 (2015).
- [12] K. Kothapalli, A. E. Böhmer, W. T. Jayasekara, B. G. Ueland, P. Das, A. Sapkota, V. Taufour, Y. Xiao, E. E. Alp, S. L. Bud'ko, P. C. Canfield, A. Kreyssig, and A. I. Goldman, *Nat. Comm.* **7**, 12728 (2016).
- [13] D. Shoenberg, *Magnetic Oscillations in Metals* (Cambridge University Press, Cambridge, England, 1984, 1984).
- [14] M. D. Watson, T. Yamashita, S. Kasahara, W. Knafo, M. Nardone, J. Béard, F. Hardy, A. McCollam, A. Narayanan, S. F. Blake, T. Wolf, A. A. Haghighirad, C. Meingast, A. J. Schofield, H. v. Löhneysen, Y. Matsuda, A. I. Coldea, and T. Shibauchi, *Phys. Rev. Lett.* **115**, 027006 (2015).
- [15] K. K. Huynh, Y. Tanabe, T. Urata, H. Oguro, S. Heguri, K. Watanabe, and K. Tanigaki, *Phys. Rev. B* **90**, 144516 (2014).
- [16] T. Terashima, N. Kikugawa, A. Kiswandhi, E.-S. Choi, J. S. Brooks, S. Kasahara, T. Watashige, H. Ikeda, T. Shibauchi, Y. Matsuda, T. Wolf, A. E. Böhmer, F. Hardy, C. Meingast, H. v. Löhneysen, M.-T. Suzuki, R. Arita, and S. Uji, *Phys. Rev. B* **90**, 144517 (2014).
- [17] I. Lifshitz and A. Kosevich, *Sov. Phys. JETP* **2**, 636 (1956).
- [18] A. McCollam, R. Daou, S. Julian, C. Bergemann, J. Flouquet, and D. Aoki, *Physica B: Condensed Matter* **359361**, 1 (2005).
- [19] S. Kasahara and *et al*, submitted (2016).
- [20] Z. R. Ye, C. F. Zhang, H. L. Ning, W. Li, L. Chen, T. Jia, M. Hashimoto, D. H. Lu, Z.-X. Shen, and Y. Zhang, *arXiv:1512.02526* (2015).
- [21] C. Liu, T. Kondo, R. M. Fernandes, A. D. Palczewski, E. D. Mun, N. Ni, A. N. Thaler, A. Bostwick, E. Rotenberg, S. L. Bud'ko, P. C. Canfield, and A. Kaminski, *Nat. Phys.* **6**, 419 (2010).
- [22] A. Audouard, F. Duc, L. Drigo, P. Toulemonde, S. Karlsson, P. Strobel, and A. Sulpice, *Europhys. Lett.* **109**, 27003 (2015).
- [23] K. Yamaji, *J. Phys. Soc. Jpn.* **58**, 1520 (1989).
- [24] The Yamaji angle caused by the interference of the maximum and minima orbits of a corrugated Fermi surface occurs when $J_0(ck_F \tan \theta_Y) = 0$, where J_0 is the Bessel function, k_F is the in-plane Fermi momentum and c is the lattice parameter.
- [25] P. Reiss and *et al*, in preparation (2017).
- [26] L. Fanfarillo, J. Mansart, P. Toulemonde, H. Cercellier, P. Le Fèvre, F. Bertran, B. Valenzuela, L. Benfatto, and V. Brouet, *Phys. Rev. B* **94**, 155138 (2016).
- [27] H. Shishido, A. F. Bangura, A. I. Coldea, S. Tonegawa, K. Hashimoto, S. Kasahara, P. M. C. Rourke, H. Ikeda, T. Terashima, R. Settai, Y. Onuki, D. Vignolles, C. Proust, B. Vignolle, A. McCollam, Y. Matsuda, T. Shibauchi, and A. Carrington, *Phys. Rev. Lett.* **104**, 057008 (2010).
- [28] A. I. Coldea, J. D. Fletcher, A. Carrington, J. G. Analytis, A. F. Bangura, J.-H. Chu, A. S. Erickson, I. R. Fisher, N. E. Hussey, and R. D. McDonald, *Phys. Rev. Lett.* **101**, 216402 (2008).
- [29] S. Hosoi, K. Matsuura, K. Ishida, H. Wang, Y. Mizukami, T. Watashige, S. Kasahara, Y. Matsuda, and T. Shibauchi, *PNAS* **113**, 8139 (2016).
- [30] L. Wang, F. Hardy, T. Wolf, P. Adelman, R. Fromknecht, P. Schweiss, and C. Meingast, *physica status solidi (b)* **1-6** (2016), [10.1002/pssb.201600153](https://doi.org/10.1002/pssb.201600153).
- [31] A. V. Chubukov, M. Khodas, and R. M. Fernandes, *arXiv:1602.05503* (2016).
- [32] S. Mukherjee, A. Kreisel, P. J. Hirschfeld, and B. M. Andersen, *Phys. Rev. Lett.* **115**, 026402 (2015).
- [33] Y. Yamakawa and H. Kontani, *arXiv:1609.09618* (2016).
- [34] S.-H. Baek, D. V. Efremov, J. M. Ok, J. S. Kim, J. van den Brink, and B. Behner, *Nat. Mater.* **14**, 210 (2015).